

# Iridium(VII)–Corrole Terminal Carbides Should Exist as Stable Compounds

Jeanet Conradie, Abraham B. Alemayehu, and Abhik Ghosh\*



Cite This: *ACS Org. Inorg. Au* 2022, 2, 159–163



Read Online

ACCESS |

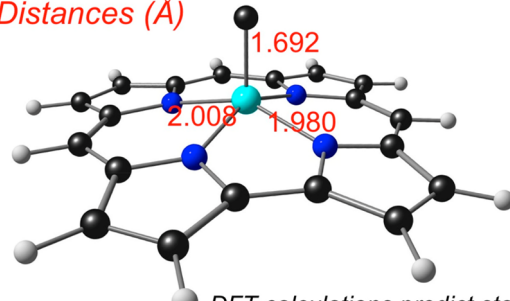
Metrics & More

Article Recommendations

Supporting Information

**ABSTRACT:** Scalar-relativistic DFT calculations with multiple exchange-correlation functionals and large basis sets foreshadow the existence of stable iridium(VII)–corrole terminal carbide derivatives. For the parent compound Ir[Cor](C), OLYP/STO-TZ2P calculations predict a short Ir–C bond distance of 1.69 Å, a moderately domed macrocycle with no indications of ligand noninnocence, a surprisingly low electron affinity of ~1.1 eV, and a substantial singlet–triplet gap of ~1.8 eV. These results, and their essential invariance with respect to the choice of the exchange-correlation functional, lead us to posit that Ir(VII)–corrole terminal carbide complexes should be isolable and indefinitely stable under ambient conditions.

Distances (Å)



DFT calculations predict stable Ir(VII)-corrole terminal carbides

**KEYWORDS:** iridium(VII), terminal carbide, carbide, high-valent, rhenium

The 5d transition metals have long provided fertile grounds for chemists' to search for ultrahigh oxidation states, thanks to the strong relativistic destabilization of the 5d orbitals.<sup>1,2</sup> Notable examples of experimentally verified ultrahigh oxidation states include the  $\text{Ir}^{\text{IX}}\text{O}_4^+$  cation,<sup>3,4</sup>  $\text{Au}^{\text{V}}\text{F}_6^-$ ,<sup>5,6</sup>  $\text{Au}^{\text{V}}_2\text{F}_{10}^-$ ,<sup>7</sup> and  $\text{Hg}^{\text{IV}}\text{F}_4$ .<sup>8</sup> Quantum chemical studies predict a number of additional as yet experimentally unconfirmed examples of such species,<sup>2</sup> as well as the 6d complexes  $\text{Rg}^{\text{VII}}\text{F}_7$ <sup>9</sup> and  $\text{Cn}^{\text{IV}}\text{F}_4$ .<sup>10</sup> In a less exotic regime, porphyrin-type ligands have long been known to stabilize high oxidation states such as Fe(IV), Mn(V), Cr(V), Ru(VI), and Os(VI). Recently, corroles have yielded rugged high-oxidation-state complexes, including  $\text{Ru}^{\text{VI}}\text{N}$ <sup>11</sup> and  $\text{Os}^{\text{VI}}\text{N}$ <sup>12,13</sup> derivatives and square-antiprismatic chiral Mo(VI)<sup>14</sup> and W(VI)<sup>15,16</sup> biscorroles. Metal oxidation states above +6, however, have proven elusive among metalloporphyrin-type complexes.<sup>17,18</sup> Thus, DFT calculations suggest that  $\text{Re}^{\text{VII}}\text{O}_2$  and  $\text{Ir}^{\text{VII}}\text{O}_2$  corrole derivatives are unlikely to exist as stable metal-dioxo species.<sup>19</sup> In a tantalizing experimental study, a putative  $\text{Re}^{\text{VII}}[\text{BCP}](\text{O})_2$  complex, where BCP<sup>3-</sup> is a trianionic benzocarbazaporphyrin ligand, turned out to be a ligand-oxidized  $\text{Re}^{\text{V}}[\text{BCPO}](\text{O})$  species instead.<sup>19</sup> DFT calculations now suggest—with a strong degree of certitude, in our considered opinion—that iridium(VII)–corrole terminal carbides should exist as stable “bottleable” species.<sup>20,21</sup>

Scalar-relativistic DFT calculations<sup>22,23</sup> (Table 1; see the Supporting Information for details) on Ir[Cor](C) with the OLYP<sup>24,25</sup> and B3LYP<sup>26,27</sup> functionals and all-electron ZORA-STO-TZ2P<sup>28,29</sup> basis sets reveal the structural and electronic hallmarks of a highly stable metallocorrole derivative. The

**Table 1. Adiabatic Electron Affinities, Singlet–Triplet Gaps, and HOMO–LUMO Gaps (eV) for Selected M(VII) Corrole Derivatives**

complex	EA		$E_{\text{S}-\text{T}}$		HOMO–LUMO gap	
	OLYP	B3LYP	OLYP	B3LYP	OLYP	B3LYP
Ir[Cor](C)	1.16	1.27	1.81	1.78	1.88	2.83
Ir[Cor](NMe) <sub>2</sub>	1.76	1.72	0.86	1.40	0.92	1.90
Re[Cor](C)	2.66	3.11	−0.17	−0.16	0.46	1.50
Re[Cor](NMe) <sub>2</sub>	2.23	2.16	0.54	0.42	0.48	0.21

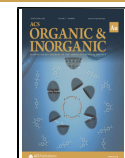
optimized structure (Figure 1), regardless of the functional, exhibits a short Ir–C distance of ~1.69 Å, which is in excellent accord with that expected on the basis of Pykkö's covalent triple-bond radii for Ir (1.07 Å) and C (0.60 Å).<sup>30–32</sup> The absence of bond length alternations in the corrole skeleton also rule out a noninnocent corrole,<sup>33–37</sup> indirectly supporting an  $\text{Ir}^{\text{VII}}\text{C}$  center. The classic Gouterman-type HOMOs,<sup>38–41</sup> with little metal character, also support the same conclusion (Figure 2). Furthermore, an almost classic corrole-based LUMO suggest a modest electron affinity (EA, Figure 3). Indeed, the calculated adiabatic EA (OLYP) turned out to be only 1.15

Received: October 3, 2021

Revised: December 6, 2021

Accepted: December 7, 2021

Published: December 14, 2021



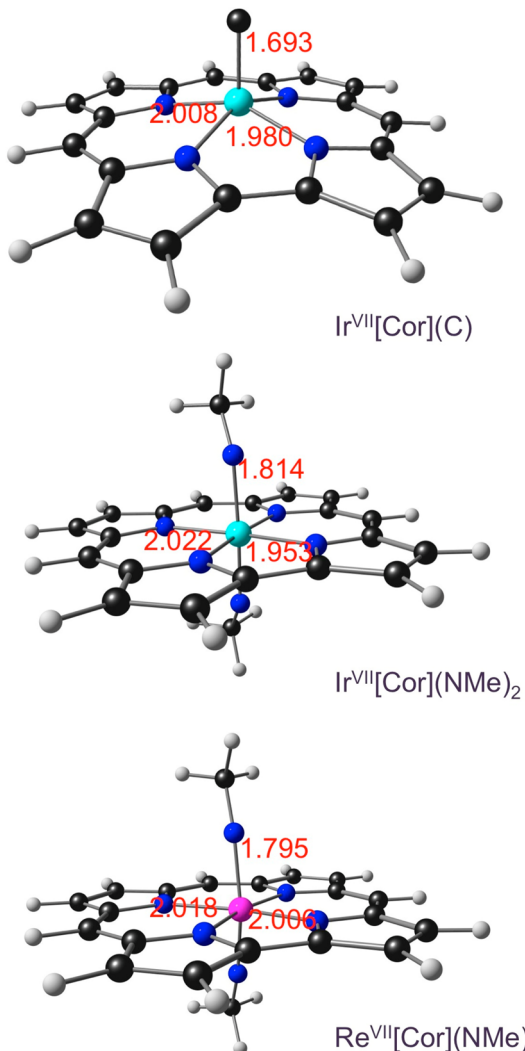


**Figure 1.** Selected M(VII) porphyrin derivatives with predicted singlet ground states.

eV, essentially the same as (or even lower than) that of a redox-innocent metalloporphyrin such as a nickel or zinc porphyrin.<sup>42,43</sup> The calculations also indicate a surprisingly large adiabatic singlet–triplet gap of 1.8 eV, another hallmark of a stable closed-shell species (Figure 3). Finally, the near-quantitative agreement between OLYP and B3LYP, two functionals, one pure and the other hybrid, that often yield divergent results,<sup>44–48</sup> greatly bolster our confidence in the calculated results, in particular our postulate that iridium(VII)–corrole terminal carbides should exist as stable “bottleable” species.<sup>49–51</sup>

Compared with  $\text{Ir}^{\text{VII}}[\text{Cor}](\text{C})$ , our calculations on  $\text{Ir}^{\text{VII}}[\text{Cor}](\text{NMe})_2$  and  $\text{Re}^{\text{VII}}[\text{Cor}](\text{NMe})_2$  indicate far higher EAs (1.78 and 2.19 eV, respectively) with OLYP, implying a much greater susceptibility to reduction and nucleophilic attack. Low adiabatic singlet–triplet gaps (0.84 and 0.67 eV, respectively) also foreshadow substantial reactivity. These differences relative to  $\text{Ir}^{\text{VII}}[\text{Cor}](\text{C})$  are primarily ascribable to lower LUMO energy levels and smaller HOMO–LUMO gaps for the two bisimido complexes. Unlike the essentially corrole-based LUMO of  $\text{Ir}^{\text{VII}}[\text{Cor}](\text{C})$ , the LUMO  $\text{Ir}^{\text{VII}}[\text{Cor}](\text{NMe})_2$  is almost exclusively localized on the  $\text{Ir}(\text{NMe})_2$  axis (Figure 3). The nature and orbital energy of the LUMO, in our view, is the

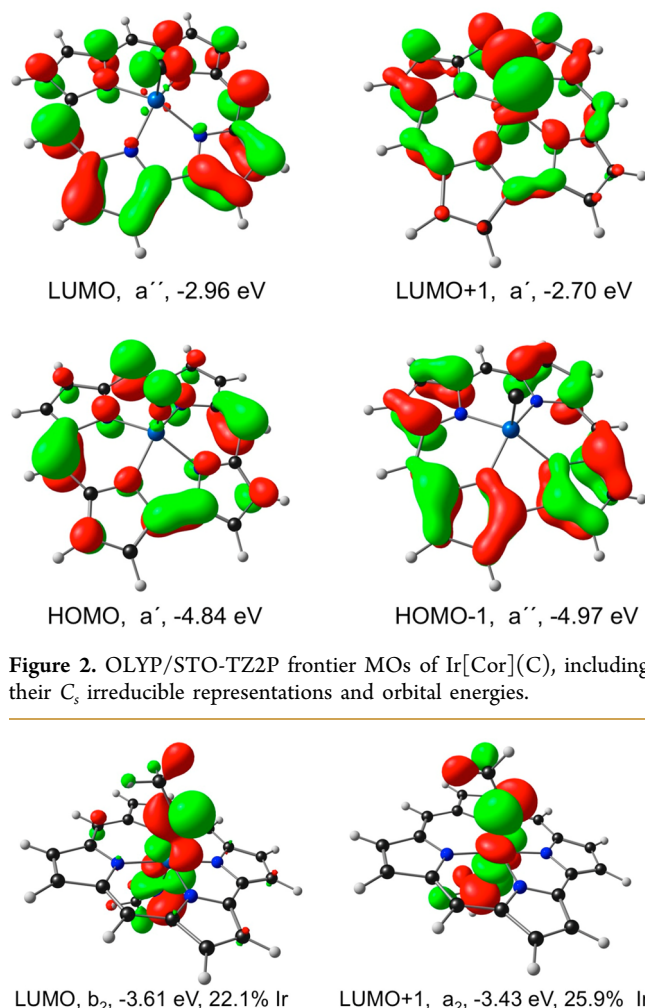


**Figure 2.** OLYP/STO-TZ2P frontier MOs of  $\text{Ir}^{\text{VII}}[\text{Cor}](\text{C})$ , including their  $C_s$  irreducible representations and orbital energies.

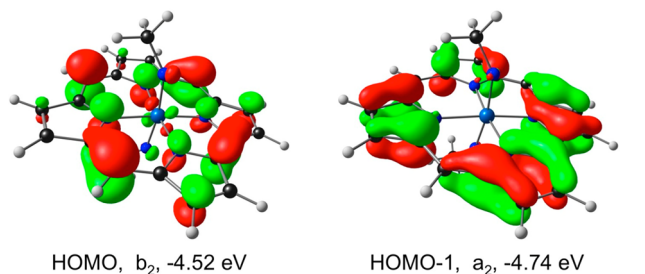


**Figure 3.** OLYP/STO-TZ2P frontier MOs of  $\text{Ir}^{\text{VII}}[\text{Cor}](\text{NMe})_2$ , including their  $C_s$  irreducible representations and orbital energies.

crux of the electronic difference between  $\text{Ir}^{\text{VII}}[\text{Cor}](\text{C})$  and  $\text{Ir}^{\text{VII}}[\text{Cor}](\text{NMe})_2$  and key to the predicted high stability of the former.

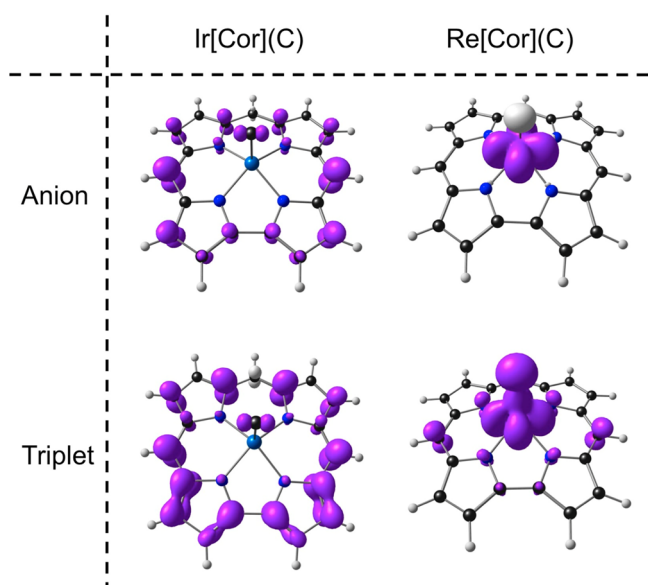
We further examined the thermodynamic stability of the three M(VII) complexes  $\text{Ir}^{\text{VII}}[\text{Cor}](\text{C})$ ,  $\text{Ir}^{\text{VII}}[\text{Cor}](\text{NMe})_2$ , and  $\text{Re}^{\text{VII}}[\text{Cor}](\text{C})$  by calculating the energetics of their reactions with  $\text{Me}_3\text{P}$  or  $\text{Me}_3\text{PO}$ , which lead to recognizably stable products (Table 2). Only electronic energies were used for this purpose. It is clear that much smaller and negative  $\Delta E$  values are associated with the reactions of  $\text{Ir}^{\text{VII}}[\text{Cor}](\text{C})$  relative to those of  $\text{Ir}^{\text{VII}}[\text{Cor}](\text{NMe})_2$  and  $\text{Re}^{\text{VII}}[\text{Cor}](\text{C})$ , clear evidence of the unique thermodynamic stability of  $\text{Ir}^{\text{VII}}[\text{Cor}](\text{C})$ .

In view of the large number of stable Re(VII) complexes known to chemists, it may seem surprising that the prospects

**Table 2. Thermochemistry of Some Hypothetical Reactions Involving Ir[Cor](C) and M[Cor](NMe)<sub>2</sub> (M = Re, Ir)**

number	reaction	$\Delta E$ (eV)		$\Delta E$ (kcal/mol)	
		OLYP	B3LYP	OLYP	B3LYP
1	Ir[Cor](C) + Me <sub>3</sub> PO → Ir[Cor](PM <sub>3</sub> ) + CO	-1.30	-1.68	-29.9	-38.7
2	Ir[Cor](C) + Me <sub>3</sub> PO → Ir[Cor](CO) + Me <sub>3</sub> P	-1.40	-1.41	-32.2	-32.6
3	Ir[Cor](C) + Me <sub>3</sub> PO → Ir[Cor](CO)(Me <sub>3</sub> P)	-1.72	-2.20	-39.6	-50.7
4	Ir[Cor](NMe) <sub>2</sub> + PMe <sub>3</sub> → Ir[Cor](Me <sub>3</sub> P) + trans-MeN=NMe	-3.11	-3.93	-71.7	-90.6
5	Re[Cor](NMe) <sub>2</sub> + PMe <sub>3</sub> → Re[Cor](NMe) + Me <sub>3</sub> P=NMe	-4.63	-6.08	-106.7	-140.2

for a stable singlet Re[Cor](C) species are almost nonexistent. Thus, both OLYP and B3LYP predict exceptionally high electron affinities >2.5 eV and negative adiabatic singlet-triplet gaps, i.e., triplet ground states (Table 1). Unlike the well-known *fac*-Re<sup>VII</sup>O<sub>3</sub><sup>52–55</sup> and [ReH<sub>9</sub>]<sup>2–</sup><sup>56–58</sup> architectures, a square-pyramidal geometry with an apical carbide simply does not bring about an adequate HOMO–LUMO gap for a stable singlet ground state; the culprit here is an exceptionally low-energy Re(d<sub>xy</sub>)-based LUMO<sup>59</sup> (which is understandable given the high Re(VII) oxidation state), which translates to the anion and triplet spin density profiles depicted in Figure 4.

**Figure 4.** OLYP/STO-TZ2P spin density plots for the anion and triplet states of Ir[Cor](C) and Re[Cor](C). Majority and minority spin densities are depicted in purple and ivory, respectively.

In summary, multiple considerations, including those of electron affinity and singlet–triplet gaps, lead us to postulate the existence of iridium(VII)–corrole carbides as highly stable species, a prediction of interest to not only high-oxidation-state chemistry but also to the field of transition metal carbides.<sup>60</sup> Terminal carbides are exceptionally rare, with only a handful of examples to date from groups 6 and 8, including  $[\{N(R)-Ar\}_3Mo(\equiv C)\}]^-$ ,  $[Tp^*(CO)_2M(\equiv CLi)]$  ( $Tp^* = 3,5$ -dimethyltris(pyrazolyl)borate; M = W, Mo),<sup>61–64</sup>  $[M(\equiv C)-L_2(X_2)]$  (M = Ru, Os),<sup>65–68</sup> and  $[P_2Mo(\equiv C)(CO)]^{+,0,-}$ .

(where P<sub>2</sub> is a terphenyl-diphosphine ligand).<sup>69,70</sup> The present predictive study, if experimentally realized, would afford the first example of a group 9 terminal carbide.

## ASSOCIATED CONTENT

### Supporting Information

The Supporting Information is available free of charge at <https://pubs.acs.org/doi/10.1021/acsorginorgau.1c00029>.

Computational methods, sample input, and optimized DFT coordinates ([PDF](#))

## AUTHOR INFORMATION

### Corresponding Author

Abhik Ghosh – Department of Chemistry, UiT The Arctic University of Norway, N-9037 Tromsø, Norway;  
ORCID: [orcid.org/0000-0003-1161-6364](https://orcid.org/0000-0003-1161-6364); Email: [abhik.ghosh@uit.no](mailto:abhik.ghosh@uit.no)

### Authors

Janet Conradie – Department of Chemistry, UiT The Arctic University of Norway, N-9037 Tromsø, Norway; Department of Chemistry, University of the Free State, Bloemfontein 9300, Republic of South Africa; ORCID: [orcid.org/0000-0002-8120-6830](https://orcid.org/0000-0002-8120-6830)

Abraham B. Alemayehu – Department of Chemistry, UiT The Arctic University of Norway, N-9037 Tromsø, Norway;  
ORCID: [orcid.org/0000-0003-0166-8937](https://orcid.org/0000-0003-0166-8937)

Complete contact information is available at:  
<https://pubs.acs.org/10.1021/acsorginorgau.1c00029>

### Notes

The authors declare no competing financial interest.

## ACKNOWLEDGMENTS

This work was supported by Grants 262229 and 324139 of the Research Council of Norway (AG) and Grants 129270 and 132504 of South African National Research Foundation.

## REFERENCES

- Pyykkö, P. Relativistic Effects in Chemistry: More Common Than You Thought. *Annu. Rev. Phys. Chem.* **2012**, *63*, 45–64.
- Hu, S.-X.; Li, W.-L.; Lu, J.-B.; Bao, J. B.; Yu, H. S.; Truhlar, D. G.; Gibson, J. K.; Marçalo, J.; Zhou, M.; Riedel, S.; Schwarz, W. H. E.; Li, J. On the Upper Limits of Oxidation States in Chemistry. *Angew. Chem., Int. Ed.* **2018**, *57*, 3242–3245.
- Wang, G.; Zhou, M.; Goettl, J. T.; Schrobilgen, G. J.; Su, J.; Li, J.; Schlöder, T.; Riedel, S. Identification of An Iridium-Containing Compound with a Formal Oxidation State of IX. *Nature* **2014**, *514*, 475–477.
- Pyykkö, P.; Xu, W. On the Extreme Oxidation States of Iridium. *Chem. - Eur. J.* **2015**, *21*, 9468–9473.
- Leary, K.; Bartlett, N. A New Oxidation State of Gold: The Preparation and Some Properties of  $[AuF_6]^-$  Salts. *J. Chem. Soc., Chem. Commun.* **1972**, *0*, 903–904.
- Leary, K.; Zalkin, A.; Bartlett, N. Crystal Structure of  $[Xe_2F_{11}]^+[AuF_6]^-$ . *J. Chem. Soc., Chem. Commun.* **1973**, *0*, 131–132.
- Hwang, I.; Seppelt, K. Gold Pentafluoride: Structure and Fluoride Ion Affinity. *Angew. Chem., Int. Ed.* **2001**, *40*, 3690–3693.
- Wang, X.; Andrews, L.; Riedel, S.; Kaupp, M. Mercury Is a Transition Metal: The First Experimental Evidence for  $HgF_4$ . *Angew. Chem., Int. Ed.* **2007**, *46*, 8371–8375.
- Ghosh, A.; Conradie, J. The Valence States of Copernicium and Flerovium. *Eur. J. Inorg. Chem.* **2016**, *2016*, 2989–2992.

- (10) Ghosh, A.; Conradie, J. The Valence States of Copernicium and Flerovium. *Eur. J. Inorg. Chem.* **2016**, *2016*, 2989–2992.
- (11) Alemayehu, A. B.; Vazquez-Lima, H.; Gagnon, K. J.; Ghosh, A. Stepwise Deoxygenation of Nitrite as a Route to Two Families of Ruthenium Corroles: Group 8 Periodic Trends and Relativistic Effects. *Inorg. Chem.* **2017**, *56*, 5285–5294.
- (12) Alemayehu, A. B.; Gagnon, K. J.; Terner, J.; Ghosh, A. Oxidative Metalation as a Route to Size-Mismatched Macroyclic Complexes: Osmium Corroles. *Angew. Chem., Int. Ed.* **2014**, *53*, 14411–14414.
- (13) Reinholdt, A.; Alemayehu, A. B.; Gagnon, K. J.; Bendix, J.; Ghosh, A. Electrophilic Activation of Osmium-Nitrido Corroles: The OsN Triple Bond as a  $\pi$ -Acceptor Metallaligand in a Heterobimetallic Os<sup>VI</sup>N–Pt<sup>II</sup> Complex. *Inorg. Chem.* **2020**, *59*, 5276–5280.
- (14) Alemayehu, A. B.; Vazquez-Lima, H.; McCormick, L. J.; Ghosh, A. Relativistic effects in metallocorroles: comparison of molybdenum and tungsten biscorroles. *Chem. Commun.* **2017**, *53*, 5830–5833.
- (15) Alemayehu, A. B.; Vazquez-Lima, H.; Gagnon, K. J.; Ghosh, A. Tungsten Biscorroles: New Chiral Sandwich Compounds. *Chem. - Eur. J.* **2016**, *22*, 6914–6920.
- (16) Schies, C.; Alemayehu, A. B.; Vazquez-Lima, H.; Thomas, K. E.; Bruhn, T.; Bringmann, G.; Ghosh, A. Metalloporphyrins as inherently chiral chromophores: resolution and electronic circular dichroism spectroscopy of a tungsten biscorrole. *Chem. Commun.* **2017**, *53*, 6121–6124.
- (17) Sanders, J. K. M.; Bamps, N.; Clyde-Watson, Z.; Darling, S. L.; Hawley, J. C.; Kim, H.-J.; Mak, C. C.; Webb, S. J. Axial Coordination Chemistry of Metalloporphyrins. In *The Porphyrin Handbook*, Vol 3; Kadish, K. M., Smith, K. M., Guillard, R., Eds.; Academic Press, 2000; pp 1–48.
- (18) Alemayehu, A. B.; Thomas, K. E.; Einrem, R. F.; Ghosh, A. The Story of 5d Metalloporphyrins: From Metal–Ligand Misfits to New Building Blocks for Cancer Phototherapeutics. *Acc. Chem. Res.* **2021**, *54*, 3095–3107.
- (19) Alemayehu, A. B.; Vazquez-Lima, H.; Teat, S. J.; Ghosh, A. Unexpected Molecular Structure of a Putative Rhodium-Dioxo-Benzocarbaporphyrin Complex. Implications for the Highest Transition Metal Valence in a Porphyrin-Type Ligand Environment. *ChemistryOpen* **2019**, *8*, 1298–1302.
- (20) For an early discussion of nonexistent molecules, focusing on compounds of low stability, see: Dasent, W. E. *Nonexistent Compounds: Compounds of Low Stability*; Marcel Dekker: New York, NY, 1965; p 185.
- (21) For a more recent discussion on nonexistent compounds that should exist, see: Hoffmann, R. Why Think Up New Molecules? *Am. Sci.* **2008**, *96*, 372.
- (22) All DFT calculations were carried out with the ADF 2020 program system,<sup>23</sup> the ZORA Hamiltonian, fine integration grids, and tight criteria for SCF cycles and geometry optimizations. In general, all energies refer to adiabatic values, i.e., differences in energy between optimized states.
- (23) te Velde, G.; Bickelhaupt, F. M.; Baerends, E. J.; Guerra, C. F.; van Gisbergen, S. J. A.; Snijders, J. G.; Ziegler, T. Chemistry with ADF. *J. Comput. Chem.* **2001**, *22*, 931–967.
- (24) Handy, N. C.; Cohen, A. Left-Right Correlation Energy. *Mol. Phys.* **2001**, *99*, 403–412.
- (25) Lee, C.; Yang, W. T.; Parr, R. G. Development of the Colle-Salvetti Correlation-Energy Formula into a Functional of the Electron-Density. *Phys. Rev. B* **1988**, *37*, 785–789.
- (26) Becke, A. D. A New Mixing of Hartree–Fock and Local Density-Functional Theories. *J. Chem. Phys.* **1993**, *98*, 1372–1377.
- (27) Stephens, P. J.; Devlin, F. J.; Chabalowski, C. F.; Frisch, M. J. Ab Initio Calculation of Vibrational Absorption and Circular Dichroism Spectra Using Density Functional Force Fields. *J. Phys. Chem.* **1994**, *98*, 11623–11627.
- (28) van Lenthe, E.; Baerends, E. J.; Snijders, J. G. Relativistic Regular Two-Component Hamiltonians. *J. Chem. Phys.* **1993**, *99*, 4597–4610.
- (29) van Lenthe, E.; Baerends, E. J.; Snijders, J. G. Relativistic Total Energy Using Regular Approximations. *J. Chem. Phys.* **1994**, *101*, 9783–9792.
- (30) Pyykkö, P.; Riedel, S.; Patzschke, M. Triple-Bond Covalent Radii. *Chem. - Eur. J.* **2005**, *11*, 3511–3520.
- (31) Pyykkö, P.; Atsumi, M. Molecular Single Bond Covalent Radii for Elements 1–18. *Chem. - Eur. J.* **2009**, *15*, 186–197.
- (32) Pyykkö, P.; Atsumi, M. Molecular Double Bond Covalent Radii for Elements Li–E112. *Chem. Eur. J.* **2009**, *15*, 12770–12779.
- (33) Ganguly, S.; McCormick, L. J.; Conradie, J.; Gagnon, K. J.; Sarangi, R.; Ghosh, A. Electronic Structure of Manganese Corroles Revisited: X-ray Structures, Optical and X-ray Absorption Spectroscopies, and Electrochemistry as Probes of Ligand Noninnocence. *Inorg. Chem.* **2018**, *57*, 9656–9669.
- (34) Vazquez-Lima, H.; Norheim, H. K.; Einrem, R. F.; Ghosh, A. Cryptic Noninnocence: FeNO Corroles in a New Light. *Dalton Trans.* **2015**, *44*, 10146–10151.
- (35) Norheim, H.-K.; Capar, J.; Einrem, R. F.; Gagnon, K. J.; Beavers, C. M.; Vazquez-Lima, H.; Ghosh, A. Ligand Noninnocence in FeNO Corroles: Insights from  $\beta$ -Octabromocorrole Complexes. *Dalton Trans.* **2016**, *45*, 681–689.
- (36) Ganguly, S.; McCormick, L. J.; Conradie, J.; Gagnon, K. J.; Sarangi, R.; Ghosh, A. Electronic Structure of Manganese Corroles Revisited: X-ray Structures, Optical and X-ray Absorption Spectroscopies, and Electrochemistry as Probes of Ligand Noninnocence. *Inorg. Chem.* **2018**, *57*, 9656–9669.
- (37) Ganguly, S.; Vazquez-Lima, H.; Ghosh, A. Wolves in Sheep's Clothing:  $\mu$ -Oxo-Diiron Corroles Revisited. *Chem. - Eur. J.* **2016**, *22*, 10336–10340.
- (38) Gouterman, M.; Wagnière, G. H.; Snyder, L. C. Spectra of Porphyrins. Part II. Four-Orbital Model. *J. Mol. Spectrosc.* **1963**, *11*, 108–115.
- (39) Gouterman, M. Optical Spectra and Electronic Structure of Porphyrins and Related Rings. In *The Porphyrins: Physical Chemistry*, Part A, Vol. 3; Dolphin, D., Ed.; Academic Press: New York, NY, 1978; pp 1–165.
- (40) For a recent biography of Martin Gouterman, see: Ghosh, A. An Exemplary Gay Scientist and Mentor: Martin Gouterman (1931–2020). *Angew. Chem., Int. Ed.* **2021**, *60*, 9760–9770.
- (41) Ghosh, A.; Wondimagegn, T.; Parusel, A. B. J. Electronic Structure of Gallium, Copper, and Nickel Complexes of Corrole. High-Valent Transition Metal Centers Versus Noninnocent Ligands. *J. Am. Chem. Soc.* **2000**, *122*, 5100–5104.
- (42) Liao, M. S.; Scheiner, S. Electronic structure and bonding in metal porphyrins, metal = Fe, Co, Ni, Cu. *J. Chem. Phys.* **2002**, *117*, 205–219.
- (43) Chen, H. L.; Ellis, P. E., Jr.; Wijesekera, T.; Hagan, T. E.; Groh, S. E.; Lyons, J. E.; Ridge, D. P. Correlation between Gas-Phase Electron Affinities, Electrode Potentials, and Catalytic Activities of Halogenated Metalloporphyrins. *J. Am. Chem. Soc.* **1994**, *116*, 1086–1089.
- (44) Conradie, J.; Ghosh, A. Electronic Structure of Trigonal-Planar Transition-Metal–Imido Complexes: Spin-State Energetics, Spin-Density Profiles, and the Remarkable Performance of the OLYP Functional. *J. Chem. Theory Comput.* **2007**, *3*, 689–702.
- (45) Conradie, J.; Ghosh, A. DFT Calculations on the Spin-Crossover Complex Fe(salen)(NO): A Quest for the Best Functional. *J. Phys. Chem. B* **2007**, *111*, 12621–12624.
- (46) Hopmann, K. H.; Conradie, J.; Ghosh, A. Broken-Symmetry DFT Spin Densities of Iron Nitrosyls, Including Roussin's Red and Black Salts: Striking Differences between Pure and Hybrid Functionals. *J. Phys. Chem. B* **2009**, *113*, 10540–10547.
- (47) Conradie, M. M.; Conradie, J.; Ghosh, A. Capturing the spin state diversity of iron(III)-aryl porphyrins: OLYP is better than TPSSh. *J. Inorg. Biochem.* **2011**, *105*, 84–91.
- (48) Sandala, G. M.; Hopmann, K. H.; Ghosh, A.; Noddleman, L. Calibration of DFT Functionals for the Prediction of <sup>57</sup>Fe Mössbauer Spectral Parameters in Iron–Nitrosyl and Iron–Sulfur Complexes:

- Accurate Geometries Prove Essential. *J. Chem. Theory Comput.* **2011**, *7*, 3232–3247.
- (49) We, however, do expect iridium–corrole carbides to act as CO-like  $\pi$ -acceptor ligands toward electron-rich transition metal centers.<sup>50,51</sup>
- (50) Reinholdt, A.; Vibenholt, J. E.; Morsing, T.ør. J.; Schau-Magnussen, M.; Reeler, N. E. A.; Bendix, J. Carbide Complexes as  $\pi$ -Acceptor Ligands. *Chem. Sci.* **2015**, *6*, 5815–5823.
- (51) Reinholdt, A.; Hill, A. F.; Bendix, J. Synthons for carbide complex chemistry. *Chem. Commun.* **2018**, *54*, 5708–5711.
- (52) Herrmann, W. A.; Herdtweck, E.; Flöel, M.; Kulpe, J.; Küsthardt, U.; Okuda, J. Organometallic oxides: the example of trioxo-( $\eta^5$ -pentamethylcyclopentadienyl)rhenium(VII). *Polyhedron* **1987**, *6*, 1165–1182.
- (53) Romão, C. C.; Kühn, F. E.; Herrmann, W. A. Rhenium(VII) Oxo and Imido Complexes: Synthesis, Structures, and Applications. *Chem. Rev.* **1997**, *97*, 3197–3246.
- (54) Conry, R. R.; Mayer, J. M. Oxygen Atom Transfer Reactions of Cationic Rhenium(III), Rhenium(V), and Rhenium(VII) Triazacyclononane Complexes. *Inorg. Chem.* **1990**, *29*, 4862–4867.
- (55) For a recent study of relativistic effects in Tc and Re complexes, see: Braband, H.; Benz, M.; Spangler, B.; Conradie, J.; Alberto, R.; Ghosh, A. Relativity as a Synthesis Design Principle: A Comparative Study of (3 + 2) Cycloaddition of Technetium(VII)- and Rhenium(VII)-Trioxo Complexes with Olefins. *Inorg. Chem.* **2021**, *60*, 11090–11097.
- (56) Abrahams, S. C.; Ginsberg, A. P.; Knox, K. Transition Metal-Hydrogen Compounds. II. The Crystal and Molecular Structure of Potassium Rhenium Hydride,  $K_2ReH_9$ . *Inorg. Chem.* **1964**, *3*, 558–567.
- (57) Parker, S. F.; Refson, K.; Williams, K. P. J.; Braden, D. A.; Hudson, B. S.; Yvon, K. Spectroscopic and Ab Initio Characterization of the  $[ReH_9]^{2-}$  Ion. *Inorg. Chem.* **2006**, *45*, 10951–10957.
- (58) Li, C.; Agarwal, J.; Schaefer, H. F. The Remarkable  $[ReH_9]^{2-}$  Dianion: Molecular Structure and Vibrational Frequencies. *J. Phys. Chem. B* **2014**, *118*, 6482–6490.
- (59) For OLYP, the HOMO and LUMO energies of  $Re[Cor](C)$  are –4.87 and –4.42 eV, respectively; for B3LYP, the corresponding values are –5.60 and –4.10 eV, respectively.
- (60) Reinholdt, A.; Bendix, J. Transition Metal Carbide Complexes. *Chem. Rev.* **2021**, DOI: 10.1021/acs.chemrev.1c00404.
- (61) Peters, J. C.; Odom, A. L.; Cummins, C. C. A Terminal Molybdenum Carbide Prepared by Methyldyne Deprotonation. *Chem. Commun.* **1997**, *20*, 1995–1996.
- (62) Enriquez, A. E.; White, P. S.; Templeton, J. L. Reactions of an Amphoteric Terminal Tungsten Methyldyne Complex. *J. Am. Chem. Soc.* **2001**, *123*, 4992–5002.
- (63) Agapie, T.; Diaconescu, P. L.; Cummins, C. C. Methine (CH) Transfer via a Chlorine Atom Abstraction/Benzene-Elimination Strategy: Molybdenum Methyldyne Synthesis and Elaboration to a Phosphaisocyanide Complex. *J. Am. Chem. Soc.* **2002**, *124*, 2412–2413.
- (64) Greco, J. B.; Peters, J. C.; Baker, T. A.; Davis, W. M.; Cummins, C. C.; Wu, G. Atomic Carbon as a Terminal Ligand: Studies of a Carbidomolybdenum Anion Featuring Solid-State  $^{13}C$  NMR Data and Proton-Transfer Self-Exchange Kinetics. *J. Am. Chem. Soc.* **2001**, *123*, 5003–5013.
- (65) Hejl, A.; Trnka, T. M.; Day, M. W.; Grubbs, R. H. Terminal ruthenium carbido complexes as  $\sigma$ -donor ligands. *Chem. Commun.* **2002**, *21*, 2524–2525.
- (66) Carlson, R. G.; Gile, M. A.; Heppert, J. A.; Mason, M. H.; Powell, D. R.; Velde, D. V.; Vilain, J. M. The Metathesis-Facilitated Synthesis of Terminal Ruthenium Carbide Complexes: A Unique Carbon Atom Transfer Reaction. *J. Am. Chem. Soc.* **2002**, *124*, 1580–1581.
- (67) Stewart, M. H.; Johnson, M. J. A.; Kampf, J. W. Terminal Carbido Complexes of Osmium: Synthesis, Structure, and Reactivity Comparison to the Ruthenium Analogues. *Organometallics* **2007**, *26*, 5102–5110.
- (68) Caskey, S. R.; Stewart, M. H.; Kivela, J. E.; Sootsman, J. R.; Johnson, M. J. A.; Kampf, J. W. Two Generalizable Routes to Terminal Carbido Complexes. *J. Am. Chem. Soc.* **2005**, *127*, 16750–16751.
- (69) Buss, J. A.; Bailey, G. A.; Oppenheim, J.; VanderVelde, D. G.; Goddard, W. A.; Agapie, T. CO Coupling Chemistry of a Terminal Mo Carbide: Sequential Addition of Proton, Hydride, and CO Releases Ethenone. *J. Am. Chem. Soc.* **2019**, *141*, 15664–15674.
- (70) Bailey, G. A.; Buss, J. A.; Oyala, P. H.; Agapie, T. Terminal, Open-Shell Mo Carbide and Carbyne Complexes: Spin Delocalization and Ligand Noninnocence. *J. Am. Chem. Soc.* **2021**, *143*, 13091–13102.